J. of Supercritical Fluids 58 (2011) 58–67

Contents lists available at ScienceDirect

The Journal of Supercritical Fluids

journal homepage: www.elsevier.com/locate/supflu

Fractionation of essential oils with biocidal activity using supercritical CO_2—Experiments and modeling

Nicolás Gañán, Esteban A. Brignole*

Planta Piloto de Ingeniería Química – PLAPIQUI, Universidad Nacional del Sur – CONICET, Camino La Carrindanga Km 7 – CC 717, Bahía Blanca, Argentina

ARTICLE INFO

Article history:
Received 23 February 2011
Received in revised form 20 April 2011
Accepted 21 April 2011

Keywords:
Supercritical extraction
Tagetes minuta
Salvia officinalis
Mentha piperita
Biocidal agents
Fractionation

ABSTRACT

Supercritical fluid extraction is an interesting alternative for the fractionation of essential oils, in order to obtain concentrates or compounds of interest. This technique requires information about the distribution of the components of the mixture between the phases present at different conditions of pressure, temperature and composition. In this work equilibrium information of three bioactive essential oils (*Salvia officinalis*, *Mentha piperita* and *Tagetes minuta* oil) with near-critical and supercritical carbon dioxide is measured using a dynamic apparatus in the range of 313–323 K and 60–120 bar. The distribution of monoterpenes, oxygenated terpenes and sesquiterpenes in the extract phase is determined by gas chromatography in order to explore the best operating conditions for the separation of the fractions or compounds with higher biocidal activity. Predictive calculations are performed using the group contribution equation of state (GC-EOS) and compared with the experimental data.

1. Introduction

Fractionation of natural complex mixtures in order to obtain pure compounds or concentrates of interest has been the subject of extensive research. The traditional methods are steam distillation (with or without vacuum), liquid solvent extraction, preparative chromatography, adsorption and selective membranes processes. The use of supercritical fluid extraction, and in particular with supercritical carbon dioxide, is an interesting alternative due to several advantages, like lower operating temperatures, preservation of thermo labile compounds and free of solvent extracts. In addition carbon dioxide is neither flammable nor toxic, allowing a safer operation. The main drawback is that relatively high pressure and large flow rates are needed, which requires optimization of the operating conditions. Comprehensive reviews have been reported by Brennecke and Eckert [1] and Diaz and Brignole [2].

In the particular case of essential oils, the supercritical deterpenation of citrus oils has been extensively studied. In this case the separation problem is the removal of hydrocarbon monoterpenes – which are unstable and generate undesired flavors – to obtain a concentrated oxygenated flavor (aroma) fraction. This fractionation, carried out continuously or semi-continuously in a packed column, notably increases oil quality and prize. Several studies have been published reporting experimental data and modeling [3–7] as well as process simulation and optimization [8,9].

The comprehensive reviews by Reverchon [10] and Reverchon and De Marco [11] covered many studies regarding the supercritical extraction of herbal essential oils. The fractionation of such oils generally appears coupled to the extraction itself. In this case, different extract fractions can be collected, from the supercritical extract, in one or more vessels operating at different temperature and/or pressure conditions. Other works deal with fractionation of raw oils or concretes, continuously or semi-continuously, both experimentally and through modeling, in order to concentrate the aroma fraction, modify its properties, or obtain compounds of interest [12,13].

Essential oils are, at the same time, complex and simple mixtures. Complex as they are composed of dozens and sometimes even hundreds of different compounds, although there can be a few predominant ones depending on species and variety. But they are also simple because their components mainly have a terpenic nature, i.e., their chemical structures are closely related and they present a high degree of isomery. This similarity, which may determine similar phase behavior, can set a limit to the selectivity of separation processes. In general three main fractions of compounds can be distinguished: hydrocarbon monoterpenes (MT), oxygenated monoterpenes (OT) and sesquiterpenes (ST), although higher order terpenes, waxes, paraffins and pigments can also be present in amounts that depend on the species and the conditions at which the oil is obtained [14].

In this work the essential oils from three species: common sage (*Salvia officinalis*), *Tagetes minuta* and peppermint (*Mentha piperita*)

* Corresponding author. Tel.: +54 2914861700; fax: +54 2914861600.
E-mail addresses: ebrignole@plapiqui.edu.ar, eabrignole@gmail.com (E.A. Brignole).

0896-8446/$ – see front matter © 2011 Elsevier B.V. All rights reserved.
doi:10.1016/j.supflu.2011.04.010

Table 1
Sage oil composition.

Component	*M* (g/mole)	%
Hydrocarbon monoterpenes (MT)		
α-Pinene	136.24	8.71
Camphene	136.24	5.54
β-Pinene	136.24	1.59
Myrcene	136.24	1.30
Other (<1%)	–	0.95
TOTAL MT		**18.09**
Oxygenated monoterpenes (OT)		
1,8-Cineol	154.25	5.27
α-Thujone	152.23	36.31
β-Thujone	152.23	7.61
Camphor	152.23	14.66
Other (<1%)	–	5.47
TOTAL OT		**69.32**
Sesquiterpenes (ST)		
α-Caryophyllene	204.36	4.04
β-Caryophyllene	204.36	4.18
Gurjunene	204.36	3.29
Other (<1%)	–	1.07
TOTAL ST		**12.58**

Table 2
Tagetes minuta oil composition.

Component	*M* (g/mole)	%
Hydrocarbon monoterpenes (MT)		
β-Pinene	136.24	1.32
D-Limonene	136.24	7.01
E-ocimene	136.24	25.97
Other (<1%)	–	0.80
TOTAL MT		**35.10**
Oxygenated monoterpenes (OT)		
Dihydrotagetone	154.25	1.72
E-tagetone	152.23	2.25
NI	–	2.33
Z-ocimenone	150.22	11.20
E-ocimenone	150.22	44.13
Other (<1%)	–	3.27
TOTAL OT		**64.90**

are studied. The fractionation of the extracts with near-critical and supercritical carbon dioxide is considered in order to obtain fractions with biocidal activity. Biocidal agents are defined as "active substances and preparations containing one or more active substances intended to destroy, deter, render harmless, prevent the action of, or otherwise exert a controlling effect on any harmful organism by chemical or biological means" [15]. The biocidal activity exhibited by many essential oils is well known. Biocidal agents are natural defense mechanisms of plants against insects, bacteria, fungi, weeds or other plants. The biocidal activity of many essential oils against different organisms has been the subject of several studies. See for example the review by Nerio et al. [16] about essential oils with activity against insects and other arthropods or the review by Zygadlo and Juliani [17].

Among the oils studied in this work, sage oil is used mainly for its flavoring properties, but also for its therapeutic attributes. For this oil 1,8-cineol (eucalyptol), thujone and camphor have been identified as their most active components against different types of bacteria [18]. Several authors have studied supercritical extraction of sage oil with carbon dioxide, for example Reverchon et al. [19], Aleksovsky and Sovová [20], Glisic et al. [21]. Glisic et al. [22] have also recently reported a work using ultrasound followed by supercritical extraction.

T. minuta oil, besides its aromatic properties, exhibits biocidal activity. This property has been studied by several researchers: Wells et al. [23] and Gillij et al. [24] have studied its mosquito repellency, Scrivanti et al. [25] and López et al. [26] have considered it as an allellopatic agent, Vasudevan et al. [27] and Singh et al. [28] have approached it from an economic point of view, and Daghero et al. [29] and Gil et al. [30] have studied its composition and extraction by traditional methods and supercritical fluids. The unsaturated terpene β-ocimene and the unsaturated ketones ocimenone, tagetone and dihydrotagetone have been identified as the components with high antimicrobial activity [31].

Peppermint oil is, after citrus oils, one of the most broadly used in the flavor and fragrance industry. Its antiseptic properties are mainly due to the presence of L-menthol [32]. Supercritical extraction of peppermint oil has been studied by several authors, for example Barton et al. [33], Reverchon et al. [34] and Roy et al. [35].

The feasibility of separation of the essential oil mixture components or fractions depends on the way the components distribute between the phases present in the separation device. This information is usually given in terms of the "relative volatility", defined as:

$$\alpha_{ij} = \frac{y_i/x_i}{y_j/x_j} = \frac{K_i}{K_j} \quad (1)$$

where y_i and x_i are the molar fractions of component "*i*" in the light and heavy phases in equilibrium, respectively, and K_i is the distribution coefficient (or K-factor). Relative volatility is, in general, a function of temperature, pressure, and composition of the mixture.

As pointed out by Diaz et al. [9], when dealing with multicomponent mixtures it is important to take into account not only the relative volatility obtained from binary information but also from ternary or multicomponent data, because mutual interaction among solutes can notably change their individual behavior. Predictions based only on binary information may be inaccurate when applied to multicomponent systems.

In the present work we experimentally studied the fractionation of sage, *T. minuta* and peppermint essential oils, using a dynamic extraction apparatus, in order to determine the equilibrium distribution of their components in near-critical and supercritical carbon dioxide, at different conditions of temperature, pressure, and composition. The equilibrium composition was also predicted using the group contribution equation of state (GC-EOS) [36]. The model predictions, in particular the predictions of relative volatilities in multicomponent mixtures, were validated by present experimental results and data reported by other authors. The best operating conditions for fractionation are selected based upon these experimental and modeling results.

2. Experimental

2.1. Materials

Sage and peppermint essential oils were extracted in PLAPIQUI by hydrodistillation from fresh plant material from Sierra de la Ventana, Argentina. They exhibit very light green colors and densities of 0.93 and 0.90 g/mL at 293 K, respectively.

T. minuta essential oil was extracted in Universidad Nacional de Cordoba, Argentina, by hydrodistillation from fresh plant material from Sierras de Cordoba. It has a strong yellow color and a density of 0.88 g/mL at 293 K.

Essential oils were stored in a freezer at 263 K. Tables 1–3 show their compositions determined by gas chromatography and mass spectrometry (GC–MS). In order to analyze and model these data, components were grouped into the three fractions mentioned above: MT, OT and ST. Sage oil contained the three fractions but *Tagetes* oil only contained significant amounts of MT and OT. In the case of peppermint oil, mainly constituted by OT, two fractions were identified: a more volatile one (F1) that includes menthofuran,

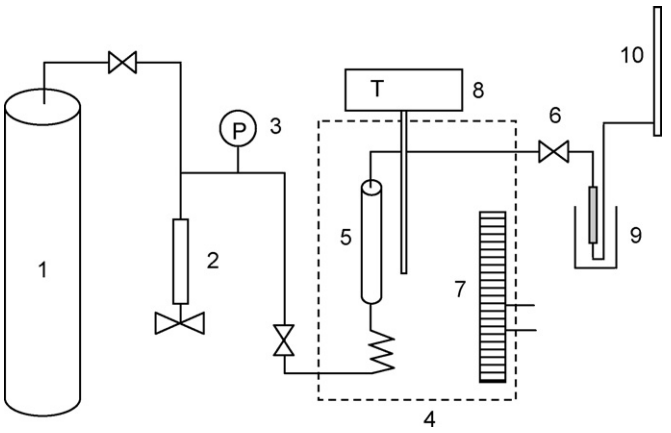

Fig. 1. Experimental apparatus. 1. CO_2 reservoir; 2. pressure generator; 3. manometer; 4. thermostatic chamber; 5. extraction column; 6. expansion valve; 7. heating resistance; 8. temperature controller; 9. collector U-tube; 10. bubble gas meter.

1,8-cineol and menthone, and a less volatile one (F2) constituted mainly by L-menthol, menthyl acetate and their isomers. In the cathegory "other" all components whose fraction is individually lower than 1% are included.

Industrial extra-dry carbon dioxide from Linde was used in the experiments. In GC analysis, chromatographic n-hexane from Aberkon Quimica and hydrogen 99.999% from Air Liquide were used.

2.2. Experimental apparatus and procedure

Experimental runs were performed in a semi continuous extraction apparatus, as shown schematically in Fig. 1. It consists of a stainless steel extraction column of 50 mL of internal volume (5) in which the essential oil sample is loaded (1.0–1.5 mL), embedded on 80-mesh glass beads. The ends of this column are filled with glass wool in order to improve solvent distribution and avoid entrainment of oil droplets. Carbon dioxide is continuously fed to the column using a pressure generator (2). Pressure and temperature in the column are kept constant. A preheating coil ensures that the carbon dioxide reaches the desired temperature before entering the column. After loading, the system is allowed to reach equilibrium conditions with all valves closed, for a period of time of no less than 2 h. At this point inlet and outlet valves are opened and the outlet flow rate is adjusted. In the outlet valve (6) the expansion of the light phase (extract) takes place. The outlet valve was wrapped with a heating tape to avoid the formation of solid particles due to the cooling effect of carbon dioxide expansion. The expanded gas goes through a collector glass U-tube (9). This tube is filled with metal and glass wool in order to increase contact area and it is immersed in a cooling bath (ethanol at 223 K) in order to minimize solute losses. Gas flow rate is measured at room temperature with a bubble gas meter (10). For each experimental run, a small sample of about 50 mg of extract is condensed to ensure that equilibrium conditions inside the cell are not perturbed. For each condition, a new sample of oil is loaded into the cell. The collected samples are weighed in a precision balance Sartorius CP224S (d = 0.1 mg), recovered with n-hexane and stored in a freezer for further chromatographic analysis. The amount of carbon dioxide consumed in each run is volumetrically determined by integrating the flow rate vs. time. Total volume is converted to mass after pertinent

Table 3
Peppermint oil composition.

Component	M (g/mole)	%
Fraction 1 (F1)		
β-pinene	136.24	1.01
Terpinyl acetate	196.29	2.57
1,8-Cineol	154.25	3.61
Isomenthone	154.25	1.30
Menthofuran	150.22	11.79
TOTAL F1		**20.27**
Fraction 2 (F2)		
Isomenthol	156.27	4.18
Menthol	156.27	26.51
Menthyl acetate	198.30	3.63
Isomenthyl acetate	198.30	44.36
β-Caryophyllene	204.36	1.05
TOTAL F2		**79.73**

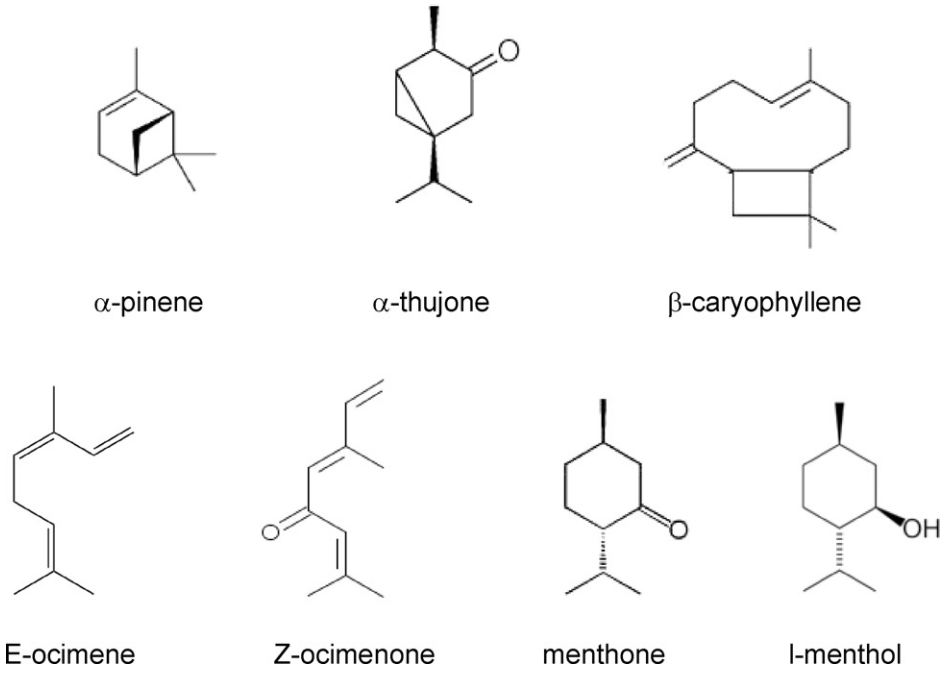

Fig. 2. Chemical structure of selected components.

Table 4
Critical properties for selected components.

Component	T_c (K)	P_c (bar)	D_c (cm/mole)[c]
α-Pinene	644.0[a]	27.6[a]	5.3167
Menthone	686.6[b]	26.0[b]	5.8165
E-ocimene	643.3[b]	24.5[b]	5.8985
α-Thujone	680.5[b]	28.8[b]	5.4496
L-Menthol	685.0[a]	20.0[a]	5.9772
Z-ocimenone	640.8[b]	26.0[b]	5.3948
β-Caryophyllene	746.3[b]	20.1[b]	6.5205
CO_2	304.2[a]	72.8[a]	3.1289

[a] Data from literature.
[b] Estimated by Joback group contribution method.
[c] Determined from a vapor pressure point.

corrections related to atmospheric pressure, temperature and humidity are taken into account.

With this apparatus the extract-phase composition and total solubility or solvent load capacity were determined at different temperature and pressure conditions for each oil. In the case of sage oil, runs were performed at 313 K and pressures in the range of 70–100 bar. In the case of *T. minuta* and peppermint oil, runs were carried out at 313 and 323 K and pressures in the range of 60–120 bar. In both cases the runs were performed at increasing pressure until homogeneous conditions were reached. Solvent flow rate was set at approximately 0.1 g/min, low enough as to obtain saturation conditions at the outlet (dynamic or "gas saturated" method). Results are discussed in Section 4.

2.3. Analysis

Analyses of the samples obtained in the experiments were performed in a Varian CX3400 gas chromatograph with a flame ionization detector (GC-FID), and a capillary column DB5-HT (Agilnet Technologies Inc., 15 m length, 0.32 mm i.d., 0.1 μm film thickness). Hydrogen was used as carrier, at a flow rate of 1 mL/min and a split ratio of 100:1. Injection temperature was fixed at 493 K and detector temperature at 543 K. The column temperature program was 318 K constant for 4 min, 8 K/min up to 513 K.

Peak identification was performed by comparison with the raw oil chromatographic profiles obtained by GC–MS under similar conditions. It was assumed that the ratio between the area of each peak and the total area (without computing the solvent peak area) was equal to the mass fraction of the corresponding component on a solvent-free basis.

3. Modeling

3.1. Thermodynamic model

Modeling of the essential oil + CO_2 systems was carried out using the group contribution equation of state (GC-EOS) [36]. This model is particularly suitable for the representation of complex mixtures of a great number of compounds using a limited number of functional groups and binary interaction parameters. This model has been previously used in several studies to describe the behavior of essential oils and other mixtures in supercritical processes [8,9,37].

The different essential oils were modeled, according to their complexity, as pseudo-binary or pseudo-ternary mixtures. For that purpose, a representative compound of each fraction, generally the most abundant one, was chosen. This approach is justified because the differences in volatility of these fractions are mainly due to the presence of polar oxygenated groups or due to their different molecular weights. α-pinene, α-thujone and β-caryophyllene were selected for the modeling of sage oil, E-ocimene and Z-ocimenone for *T. minuta* oil and menthone and L-menthol for peppermint oil. Table 4 shows the critical temperature, pressure and critical diameter of these components. Fig. 2 shows their molecular structures.

The parameter matrix of the GC-EOS, with its successive extensions and revisions, was used [9,38,39]. As the binary interaction parameters between the ketone group and the different olefinic groups were not available, they were determined by correlation of vapor pressure data of the unsaturated ketones dihydrocarvone [14], 4-methyl-3-penten-2-one [40] and 5-hexen-2-one [41] and experimental vapor–liquid equilibrium data of binary systems (olefin + ketone): 1-hexene + 2-butanone [42], 2-methyl-2-butene + 2-butanone [43], 2-methyl-2-butene + methyl isopropyl ketone [43], isoprene + methyl isopropyl ketone [43]. Tables 5–8 show the GC-EOS component group compositions, pure group parameters, and binary interaction parameters for the selected components. Only the pure group parameters for the ketone group of ocimenone had to be modified in order to compute the lack of a hydrogen atom in the adjacent carbon atom.

The experimental information obtained in the present work was not included in the parameter estimation of the model; therefore all the calculations are completely predictive. Experimental vapor

Table 6
Pure group parameters.

Group	T^* (K)	q	g^*	g'	g''
CH_3	600	0.848	316,910	−0.9274	0
CH_2	600	0.540	356,080	−0.8755	0
CH	600	0.228	356,080	−0.8755	0
CH_3(B)	600	0.789	316,910	−0.9274	0
$CYCH_2$	600	0.540	466,550	−0.6062	0
CYCH	600	0.228	466,550	−0.6062	0
$CH{=}CH_2$	600	1.176	337,980	−0.6764	0
$C{=}CH_2$	600	0.988	323,440	−0.6328	0
C=CH	600	0.676	546,780	−1.0966	0
$CH_2C{=}O$	600	1.18[a]	888,410	−0.7018	0
CHOH	512.6	0.908	1,207,500	−0.6441	0
CO_2	304.2	1.261	531,890	−0.5780	0

[a] q = 0.88 in ocimenone

Table 5
GC-EOS group composition for selected components.

Group	α-Pinene	α-Thujone	β-Caryophyllene	Ocimene	Ocimenone	Menthone	Menthol	CO_2
CH_3	1	3	1	3	3	3	3	–
CH_2	–	–	–	1	–	–	–	–
CH	–	1	–	–	–	1	1	–
CH_3(B)	2	–	2	–	–	–	–	–
$CYCH_2$	2	1	5	–	–	2	3	–
CYCH	2	2	2	–	–	2	2	–
$CH{=}CH_2$	–	–	–	1	1	–	–	–
$C{=}CH_2$	–	–	1	–	–	–	–	–
C=CH	1	–	1	2	1	–	–	–
$CH_2C{=}O$	–	1	–	–	1	1	–	–
CHOH	–	–	–	–	–	–	1	–
CO_2	–	–	–	–	–	–	–	1

Table 7
Binary interaction parameters (k_{ij} above diagonal, k'_{ij} below diagonal).

Group	CH_3	CH_2	CH	CH_3(B)	$CYCH_2$	CYCH	$CH{=}CH_2$	$C{=}CH_2$	C=CH	$CH_2C{=}O$	CHOH	CO_2
CH_3	1	1	1	1	1	1	0.977	1	0.977	0.834	0.715	0.898
CH_2	0	1	1	1	1	1	0.977	n.a	0.977	0.834	n.a	0.898
CH	0	0	1	1	1	1	n.a	1	0.977	0.834	0.682	0.898
CH_3(B)	0	0	0	1	1	1	n.a	1	0.977	0.834	n.a.	0.928
$CYCH_2$	0	0	0	0	1	1	n.a	1.04	1	0.870	0.722	0.928
CYCH	0	0	0	0	0	1	n.a	1.04	1	0.870	0.722	0.928
$CH{=}CH_2$	0	0	n.a	n.a	n.a	n.a	1	n.a	1.094	n.a	n.a	0.948
$C{=}CH_2$	0	n.a.	0	0	0	0	n.a	1	1.094	1	n.a	1.057
C=CH	0	0	0	0	0	0	0	0	1	0.975	n.a	1
$CH_2C{=}O$	0.084	0.084	0.084	0.084	0.097	0.097	n.a	0	0	1	0.953	1.025
CHOH	0	n.a.	0	n.a.	0	0	n.a	n.a	n.a	0	1	0.985
CO_2	0	0	0	0	0.210	0.21	0	0	0	0.108	0	1

n.a. = not necessary for calculations.

Table 8
Binary non-randomness parameters (α_{ij} above diagonal, α_{ji} below diagonal).

Group	CH_3	CH_2	CH	CH_3(B)	$CYCH_2$	CYCH	$CH{=}CH_2$	$C{=}CH_2$	C=CH	$CH_2C{=}O$	CHOH	CO_2
CH_3	0	0	0	0	0	0	0	0	0	0.854	1.471	4.683
CH_2	0	0	0	0	0	0	0	n.a.	0	0.854	n.a.	4.683
CH	0	0	0	0	0	0	n.a.	0	0	0.854	1.471	4.683
CH_3(B)	0	0	0	0	0	0	n.a.	0	0	0.854	n.a.	4.683
$CYCH_2$	0	0	0	0	0	0	n.a.	0	0	0.854	1.471	0
CYCH	0	0	0	0	0	0	n.a.	0	0	0.854	1.417	0
$CH{=}CH_2$	0	0	n.a.	n.a.	n.a.	n.a.	0	n.a.	0	n.a.	n.a.	0
$C{=}CH_2$	0	n.a.	0	0	0	0	n.a.	0	0	0	n.a.	0
C=CH	0	0	0	0	0	0	0	0	0	0	n.a.	0
$CH_2C{=}O$	5.146	5.146	5.146	5.146	5.146	5.146	n.a.	0	0	0	0	0.17
CHOH	10.22	n.a.	10.22	n.a.	10.22	10.22	n.a.	n.a.	n.a.	0	0	−0.39
CO_2	4.683	4.683	4.683	4.683	0	0	0	0	0	0.17	0.468	0

n.a. = not necessary for calculations.

pressure data were taken from Guenther [14] and Perry [44] and are compared with GC-EOS predictions in Fig. 3. A good agreement is observed between experimental data and model predictions in the range of temperature studied. Experimental vapor pressure data for ocimene and ocimenone were not found in the open literature.

Solubility predictions of the selected components in near-critical and supercritical carbon dioxide were also verified against binary experimental data from other authors. Solubility data of α-pinene [45,46], thujone [47] and L-menthol [48–50] in carbon dioxide are compared with GC-EOS predictions in Figs. 4–6. A good agreement is observed with the exception of menthol solubility. In this case the experimental data reported by different authors present great discrepancy as indicated by Sovová et al. [49]. The GC-EOS underestimates menthol solubility in all cases. Predictions could be improved by including solute-solute association effects in the model. No information about ocimene or ocimenone solubility was found in the literature.

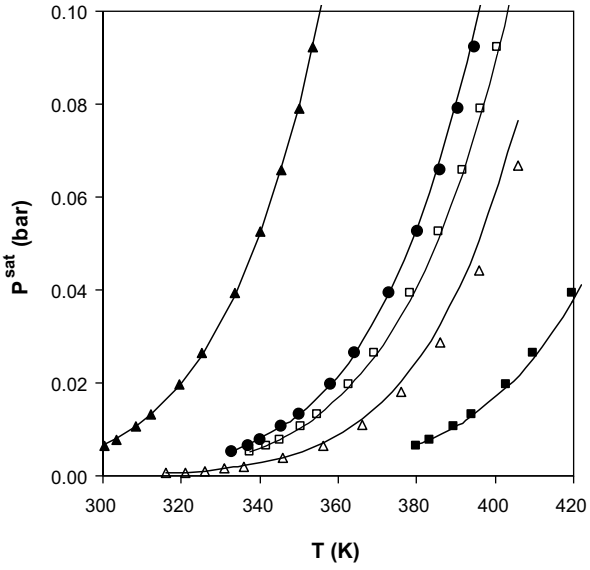

Fig. 3. Vapor pressure of selected components. (▲) α-Pinene, (●) α-thujone, (■) β-caryophyllene, (□) menthone, (△) L-menthol, and (-) GC-EOS prediction.

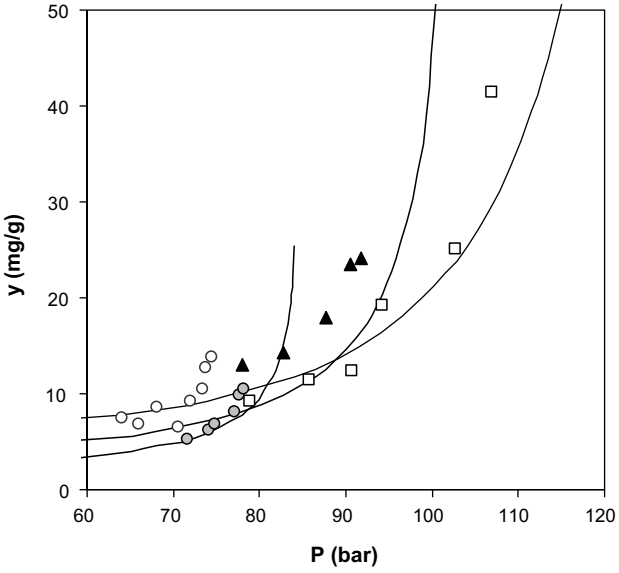

Fig. 4. Solubility of α-pinene in near critical and supercritical CO_2. (○) T = 313 K [34], (●) T = 313 K [35], (▲) T = 323 K [35], (□) T = 333 K [35], and (-) GC-EOS prediction.

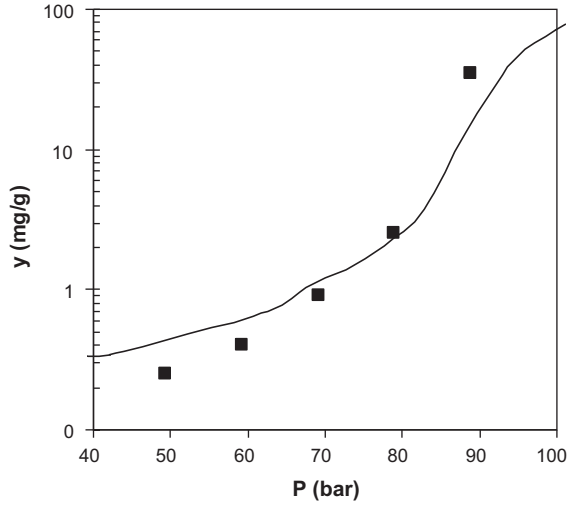

Fig. 5. Solubility of thujone in near critical and supercritical CO_2 (T = 313 K). (■) Experimental data [36] and (-) GC-EOS prediction.

4. Results and discussion

4.1. Global solubility

The experimental essential oil total solubility (or solvent load capacity) increases with pressure, as shown in Fig. 7(a–c). The solubility increase is of one order of magnitude over the pressure range studied in the present work. In the case of peppermint oil an inversion in solubility behavior is observed, as a consequence of the opposite effects of pressure and temperature on solvent density, and therefore on its solvent power. This is the well-known "cross-over" phenomenon. In Fig. 8(a–c) the solubility data are plotted as a function of pure solvent density (instead of pressure), so that the effects of pressure and temperature can be seen separately.

4.2. Extract phase composition

Tables 9–11 show the distribution of MT, OT and ST fractions for sage and *T. minuta* oil and F1 and F2 for peppermint oil in a solvent-free basis as a function of pressure for the studied

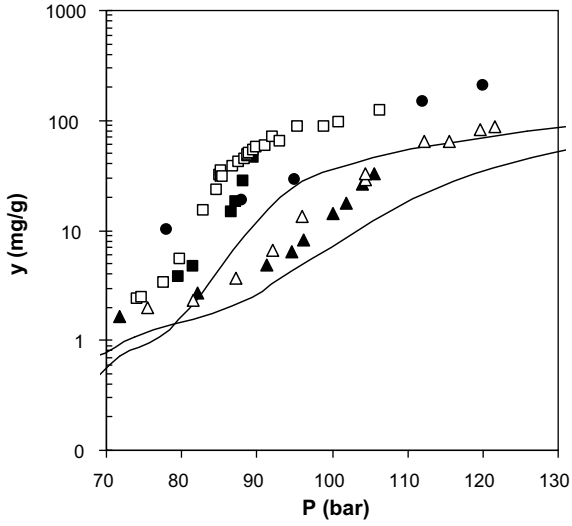

Fig. 6. Solubility of L-menthol in near critical and supercritical CO_2. (■) T = 313 K [37], (□) T = 313 K [38], (▲) T = 323 K [37], (△) T = 323 K [38], (●) T = 323 K [39], and (-) GC-EOS prediction.

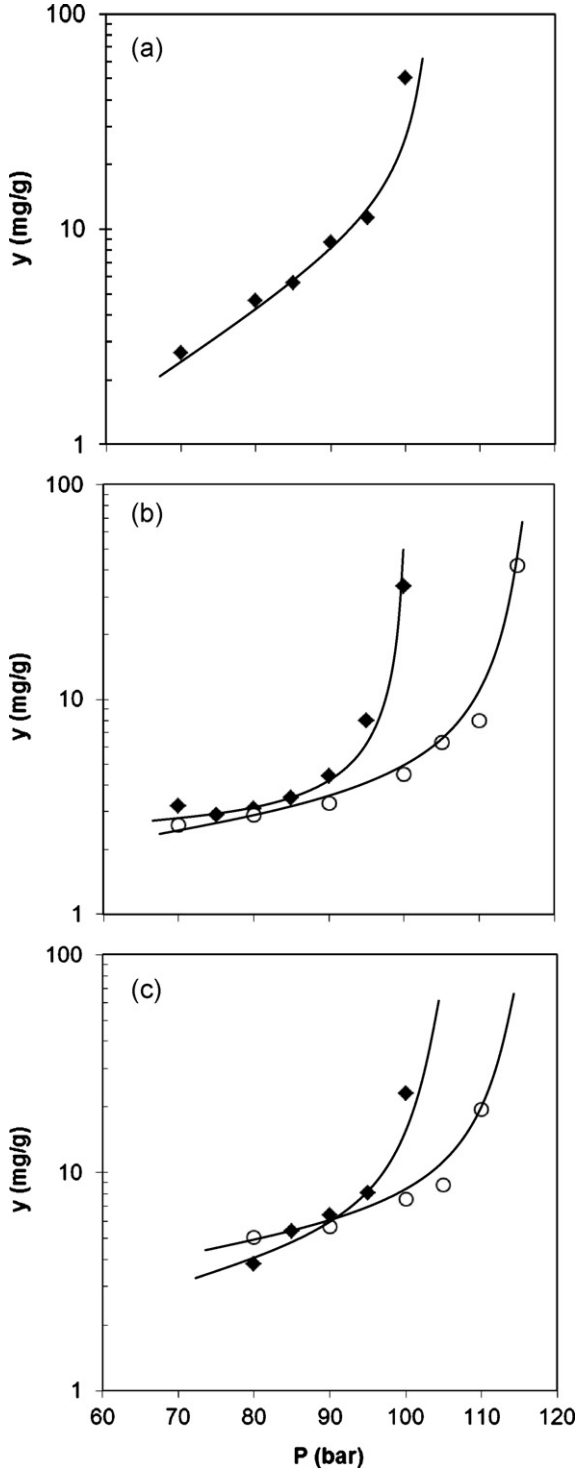

Fig. 7. Global solubility of (a) sage oil, (b) *Tagetes* oil, (c) peppermint oil in extract phase vs. pressure. (♦) T = 313 K, (○) T = 323 K, and (-) smoothed line.

Table 9
Extract-phase composition for sage oil as a function of pressure (mass fraction in solvent free basis, T = 313 K).

P (bar)	MT	OT	ST
70	0.514	0.474	0.012
80	0.489	0.503	0.008
85	0.451	0.546	0.002
90	0.365	0.615	0.020
95	0.281	0.682	0.037
Feed	0.181	0.693	0.126

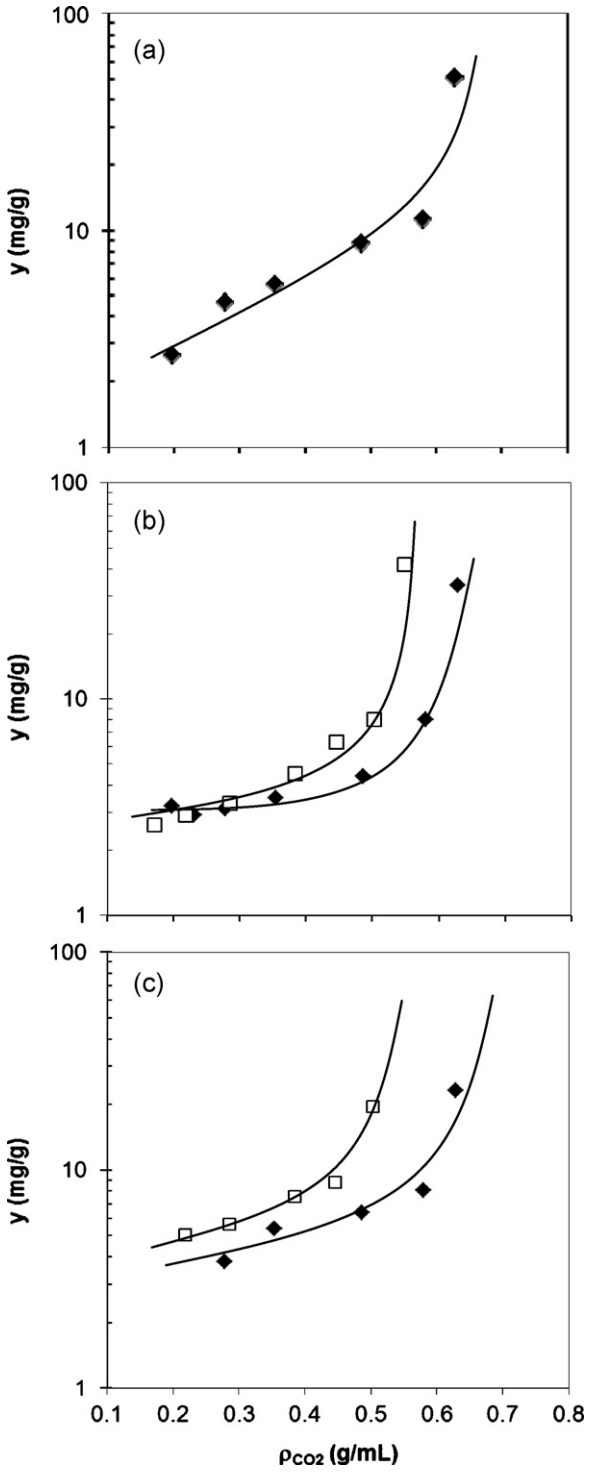

Fig. 8. Global solubility of (a) sage oil, (b) *Tagetes* oil, and (c) peppermint oil in extract phase vs solvent density. (⧫) T = 313 K, (□) T = 323 K, and (-) smoothed line.

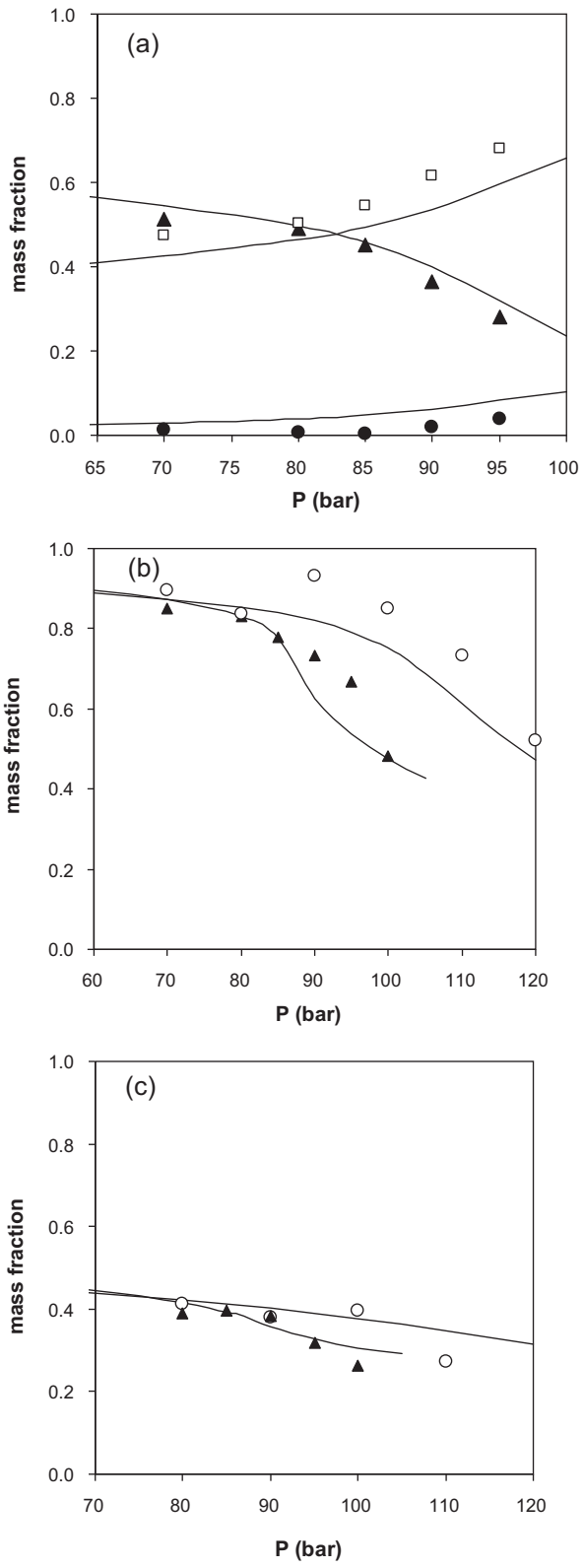

Fig. 9. (a) Extract phase composition (solvent free basis) for sage oil, T = 313 K. (▲) MT, (□) OT, (●) ST, and (-) GC-EOS prediction. (b) Extract phase composition (MT in solvent free basis) for *Tagetes* oil (▲) T = 313 K, (○) T = 323 K, and (-) GC-EOS prediction. (c) Extract phase composition (MT in solvent free basis) for peppermint oil. (▲) T = 313 K, (○) T = 323 K, and (-) GC-EOS prediction.

temperatures. In all cases extracts are richer in MT (or F1) than the raw oil, which can be expected as a consequence of the higher volatility of these fractions. It can also be seen that MT (or F1) concentration decreases with pressure, approaching the raw oil composition as the system approaches homogeneous conditions. These results and GC-EOS predictions are plotted in Fig. 9(a–c). In the case of sage oil the solvent-free extract phase composition of the three fractions is shown, while for *T. minuta* and peppermint oil only the more volatile fraction is shown. The predictions are performed

Table 10
Extract-phase composition for *Tagetes minuta* oil as a function of pressure (mass fraction in solvent free basis).

T (K)	*P* (bar)	MT	OT
313	70	0.849	0.151
	75	0.810	0.190
	80	0.830	0.170
	85	0.779	0.221
	90	0.732	0.268
	95	0.667	0.333
	100	0.480	0.520
323	70	0.895	0.105
	80	0.837	0.163
	90	0.932	0.068
	100	0.851	0.149
	110	0.733	0.267
Feed		0.351	0.649

solving a flash calculation at fixed temperature and pressure with the software GC-THREE [51]. The feed composition used in each calculation is the global composition of the respective experimental system for each run. It can be seen that the model accurately predicts the composition of the extract phase.

The results suggest that the separation between fractions F1 and F2 in peppermint oil is the most difficult to achieve: in fact, it can be seen that the extract-phase composition is similar to that of the raw oil. The relatively similar vapor pressure of menthone and L-menthol (see Fig. 3) helps to explain the difficulty in separating these two fractions.

The effect of temperature on extract-phase composition can be seen in the runs performed with *Tagetes* and peppermint oils. Results indicate that increasing temperature from 313 K to 323 K does not considerably affect the extract composition at lower pressures; the main effect is to extend the two-phase region over a higher range of pressure, allowing operation in conditions of higher solubility.

4.3. Selectivity, binary and multicomponent volatility

The analysis of the experimental data suggests that there is a tradeoff between process selectivity and solvent capacity. In order to achieve a higher degree of separation between MT and OT it is necessary to operate at relatively lower pressures (70–80 bar), range in which solvent density (and solvent power) is lower, thus requiring a high flow rate of carbon dioxide.

As mentioned above, the relative volatility between components is a measure of the selectivity in a separation process. Fig. 10(a–c) shows the experimental and predicted relative volatilities of MT vs. non-MT (or F1 vs. F2) as a function of pressure for the studied oils. Experimental values are calculated from the extract phase composition and the heavy phase composition is estimated

Table 11
Extract-phase composition for peppermint oil as a function of pressure (mass fraction in solvent-free basis).

T (K)	*P* (bar)	F1	F2
313	80	0.390	0.610
	85	0.396	0.604
	90	0.384	0.616
	95	0.319	0.681
	100	0.263	0.737
323	80	0.411	0.589
	90	0.379	0.621
	100	0.397	0.603
	110	0.272	0.728
Feed		0.203	0.797

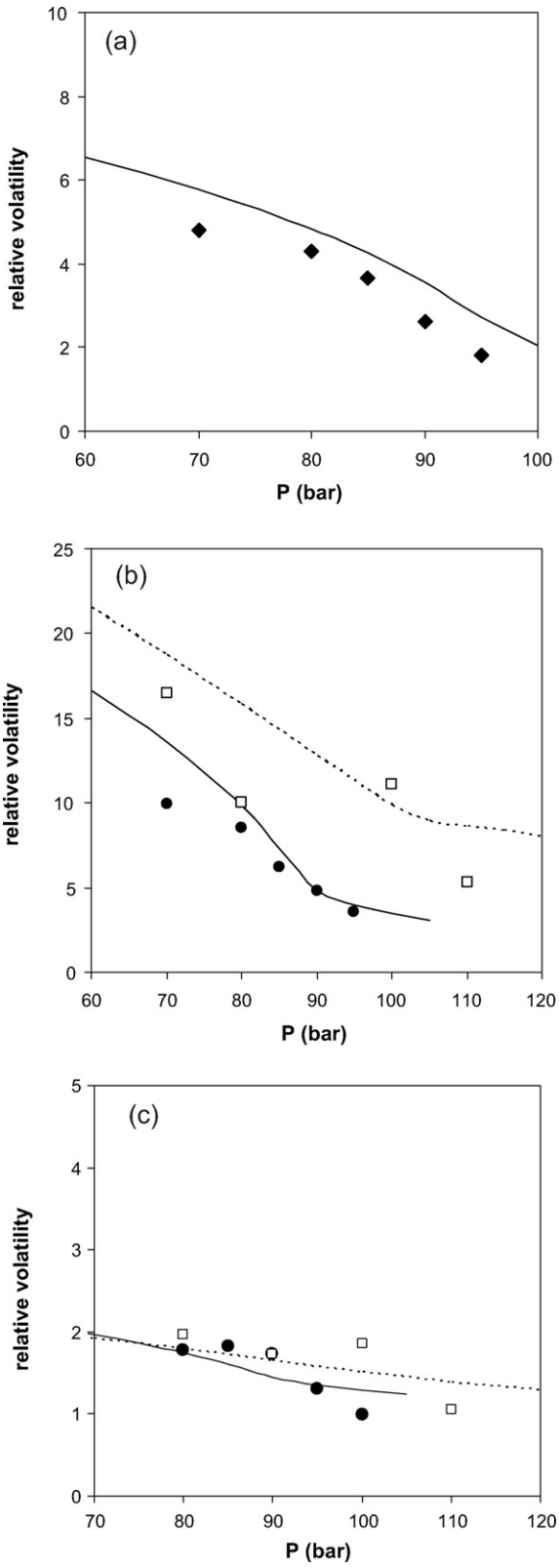

Fig. 10. (a) Relative volatility of MT vs. non-MT for sage oil (T = 313 K). (♦) experimental value (this work) and (-) GC-EOS prediction. (b) Relative volatility of MT vs. OT for *Tagetes* oil. (●) T = 313 K, experimental value (this work), (□) T = 323 K, experimental value (this work), (-) T = 313 K, GC-EOS prediction, and (- -) T = 323 K, GC-EOS prediction. (c) Relative volatility of F1 vs. F2 for peppermint oil. (●) T = 313 K, experimental value (this work), (□) T = 323 K, experimental value (this work), (-) T = 313 K, GC-EOS prediction, (- -) T = 323 K, GC-EOS prediction.

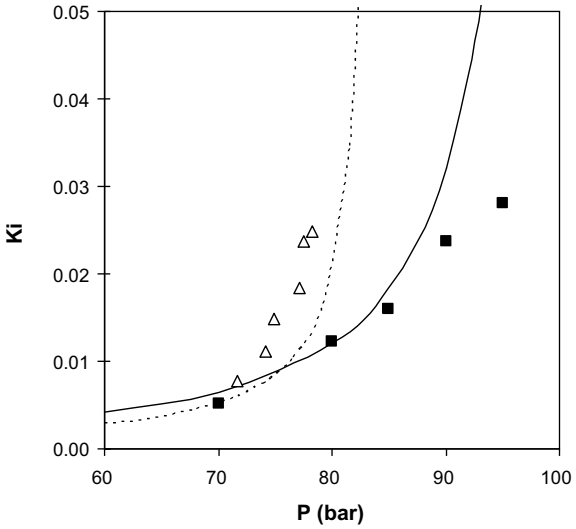

Fig. 11. Distribution coefficient (K_i) of α-pinene in carbon dioxide at T = 313 K. Binary: (△) experimental value [35], (- -) GC-EOS prediction. Multicomponent: (■) experimental value (this work) and (-) GC-EOS prediction.

to be equal to the raw oil composition corrected by the amount of carbon dioxide dissolved in it. It can be seen that in all cases the highest values are achieved at lower pressures.

Three other different phenomena can also be observed. The separation degree for *Tagetes* oil is high and therefore it can be more easily fractionated, obtaining a relatively pure OT fraction without important losses in the extract phase. A simple counter-current column could be sufficient to obtain fractions of high purity. On the other hand, peppermint oil exhibits the most difficult separation. Relative volatility values are low in the complete range. As an intermediate case, sage oil presents a limited separation degree and suggests a more complex scheme of interactions due to the presence of a significant amount of ST. This phenomenon is also discussed in a recent work mentioned earlier [22]. Such behavior could not have been correctly predicted using only binary information, as mentioned above. The volatility of each component (represented by the distribution coefficient or K-factor) is affected by the presence of the other components, and this effect can be significant. For example, Fig. 11 shows the experimental and predicted distribution coefficients of α-pinene – the main component of the MT fraction – in binary mixtures with carbon dioxide [35] and in the multicomponent system studied in this work, computed from the individual chromatographic results for α-pinene. In this case an important change in its volatility behavior above 80 bar can be observed. The presence of higher amounts of ST in the extract phase, due to the higher solvent density, extends the two-phase region to higher pressures, at which α-pinene is totally miscible with carbon dioxide in binary mixtures. The behavior of this particular component can be extended to the other components of the MT fraction.

5. Conclusions

The total solubility of three essential oils in near-critical and supercritical CO_2, as a function of pressure and temperature, was measured together with the distribution of the main fractions (MT, OT, ST, F1 and F2) of the essential oils in their extracts.

The GC-EOS model gave good correlations of the essential oil component vapor pressures and good predictions of their relative volatilities.

The purification of the active biocidal fraction of the *T. minuta* essential oil is quite good and can be carried out in a semi-continuous process or in a simple countercurrent column without reflux. The separation of the sage essential oil active components requires a more complex fractionation and the separation of peppermint fractions is no feasible by near-critical extraction with CO_2.

Significant variation of relative volatilities in the multicomponent mixture with respect to the values reported for binary mixtures was observed.

Acknowledgements

This work was carried thanks to the financial support of SECYT (Universidad Nacional de Córdoba), FONCYT and CONICET, Argentina. The authors thank Prof. Dr. Julio Zygadlo for providing the samples of *T. minuta* essential oil.

References

[1] J.F. Brennecke, C.A. Eckert, Phase equilibria for supercritical fluid process design, American Institute of Chemical Engineers Journal 35 (1989) 1409–1427.
[2] M.S. Diaz, E.A. Brignole, Modeling and optimization of supercritical fluid processes (review), J. Supercritical Fluids 47 (2009) 611–618.
[3] F. Temelli, J.P. O'Connell, C.S. Chen, R.J. Braddock, Thermodynamic analysis of supercritical carbon dioxide extraction of terpenes from cold-pressed orange oil, Industrial and Engineering Chemistry Research 29 (1990) 618–624.
[4] M. Budich, S. Heilig, T. Wesse, V. Leibkuchler, G. Brunner, Countercurrent deterpenation of citrus oil with supercritical CO_2, J. Supercritical Fluids 14 (1999) 105–114.
[5] F. Benvenuti, F. Gironi, L. Lamberti, Supercritical deterpenation of lemon oil, experimental data and simulation of the semicontinuous extraction process, J. Supercritical Fluids 20 (2001) 29–44.
[6] M. Kondo, N. Akgun, M. Goto, A. Kodama, T. Hirose, Semi-batch operation and countercurrent extraction by supercritical CO_2 for the deterpenation of lemon oil, J. Supercritical Fluids 23 (2002) 21–27.
[7] F. Gironi, M. Maschietti, Supercritical carbon dioxide fractionation of lemon oil by means of a batch process with an external reflux, J. Supercritical Fluids 35 (2005) 227–234.
[8] S. Espinosa, S. Diaz, E.A. Brignole, Optimal design of supercritical fluid processes, Computers and Chemical Engineering 24 (2000) 1301–1307.
[9] S. Diaz, S. Espinosa, E.A. Brignole, Citrus peel oil deterpenation with supercritical fluids. Optimal process and solvent cycle design, J. Supercritical Fluids 35 (2005) 49–61.
[10] E. Reverchon, Supercritical fluid extraction and fractionation of essential oils and related products, J. Supercritical Fluids 10 (1997) 1–37.
[11] E. Reverchon, I. De Marco, Supercritical fluid extraction and fractionation of natural matter, J. Supercritical Fluids 38 (2006) 146–166.
[12] O. Kose, U. Akman, O. Hortacsu, Semi-batch deterpenation of origanum oil by dense carbon dioxide, J. Supercritical Fluids 18 (2000) 49–63.
[13] S. Varona, A. Martin, M.J. Cocero, T. Gamse, Supercritical carbon dioxide fractionation of Lavandin essential oil: experiments and modeling, J. Supercritical Fluids 45 (2008) 181–188.
[14] E. Guenther, The Essential Oils, Volume 1, Third Printing, D. Van Nostrand Company, New York, 1957, pp. 17–83.
[15] Directive 98/8/EC of the European Parliament and of the Council of 16 February 1998 concerning the placing of biocidal products on the market, Official Journal of the European Communities.
[16] L.S. Nerio, J. Olivero-Verbel, E. Stashenko, Repellent activity of essential oils: a review, Bioresource Technology 101 (2010) 372–378.
[17] J.A. Zygadlo, H.R. Juliani, Bioactivity of essential oil components, Current Topics in Phytochemistry 3 (2000) 203–214.
[18] A.P. Longaray Delamare, I. Moschen-Pistorello, L. Artico, L. Atti-Serafini, S. Echeverrigaray, Antibacterial activity of the essential oils of *Salvia officinalis* L. and *Salvia triloba* L. cultivated in South Brazil, Food Chemistry 100 (2007) 603–608.
[19] E. Reverchon, R. Taddeo, G. Della Porta, Extraction of sage oil by supercritical CO_2: influence of some process parameters, J. Supercritical Fluids 8 (1995) 302–309.
[20] S.A. Aleksovsky, H. Sovová, Supercritical CO_2 extraction of *Sage officinalis* L., J. Supercritical Fluids 40 (2007) 239–245.
[21] S. Glisic, J. Ivanovic, M. Ristic, D. Skala, Extraction of sage (*Salvia officinalis* L.) by supercritical CO_2: kinetic data, chemical composition and selectivity of diterpenes, J. Supercritical Fluids 52 (2010) 62–70.
[22] S. Glisic, M. Ristic, D. Skala, The combined extraction of sage (*Salvia officinalis* L.): ultrasound followed by supercritical CO_2 extraction, Ultrasonics Sonochemistry 18 (2011) 318–326.
[23] C. Wells, W. Bertsch, M. Perich, Isolation of volatiles with insecticidal properties from the genus *Tagetes* (marigold), Chromatographia 34 (1992) 241–248.
[24] Y.G. Gillij, R.M. Gleiser, J.A. Zygadlo, Mosquito repellent activity of essential oils of aromatic plants growing in Argentina, Bioresource Technology 99 (2008) 2507–2515.
[25] L.R. Scrivanti, M.P. Zunino, J.A. Zygadlo, *Tagetes minuta* and *Schinus areira* essential oils as allelopathic agents, Biochemical Systematics and Ecology 31 (2003) 563–572.

[26] M.L. López, N.E. Bonzani, J.A. Zygadlo, Allelopathic potential of *Tagetes minuta* terpenes by a chemical, anatomical and phytotoxic approach, Biochemical Systematics and Ecology 36 (2009) 882–890.
[27] P. Vasudevan, S. Kashyap, S. Sharma, Tagetes: a multipurpose plant, Bioresource Technology 62 (1997) 29–35.
[28] V. Singh, B. Singh, V.K. Kaul, Domestication of wild marigold (*Tagetes minuta* L.) as a potential economic crop in Western Himalaya and North Indian plains, Economic Botany 57 (2003) 535–544.
[29] J. Daghero, M. Mattea, E. Reverchon, G. Della Porta, F. Senatore, Isolation of *Tagetes minuta* L. oil using supercritical extraction, Acta Horticulturae 4 (503) (1999) 21–25.
[30] A. Gil, C.M. Ghersa, S. Leicach, Essential oil yield and composition of *Tagetes minuta* accessions from Argentina, Biochemical Systematics and Ecology 28 (2000) 561–574.
[31] J.A. Soule, *Tagetes minuta*: a potential new herb from South America, in: J. Janick, J.E. Simon (Eds.), New Crops, Wiley, New York, 1993.
[32] G. Iscan, N. Kirimer, M. Kurkcuoglu, K.H. Can, F. Baser, Demirci, Antimicrobian screening of *Mentha piperita* essential oils, J. Agricultural and Food Chemistry 50 (2002) 3943–3946.
[33] P. Barton, R.E. Hughes Jr., M.M. Hussein, Supercritical carbon dioxide extraction of peppermint and spearmint, J. Supercritical Fluids 5 (1992) 157–162.
[34] E. Reverchon, A. Ambruosi, F. Senatore, Isolation of peppermint oil using supercritical CO_2 extraction, Flavour and Fragrance Journal 9 (1994) 19–23.
[35] B.C. Roy, M. Goto, A. Kodama, T. Hirose, Supercritical CO_2 extraction of essential oils and cuticular waxes from peppermint leaves, J. Chemical Technology and Biotechnology 67 (1996) 21–26.
[36] S. Skjold-Jorgensen, Group contribution equation of state (GC-EOS): a predictive method for phase equilibrium computations over wide ranges of temperatures and pressures up to 30 MPa, Industrial and Engineering Chemistry Research 27 (1988) 110.
[37] S. Espinosa, S.B. Bottini, E.A. Brignole, Process analysis and phase equilibria for the removal of chemicals from fatty oils using near-critical solvents, Industrial and Engineering Chemistry Research 39 (2000) 3024–3033.
[38] J. Pusch, J. Schmelzer, Extension of the group-contribution equation of state parameter matrix for the prediction of phase equilibria containing argon, ammonia, propene and other alkenes, Berichte der Bunsengesellschaft für Physikalische Chemie 97 (1993) 597.
[39] T. Fornari, Revision and summary of the group contribution equation of state parameter table: application to edible oil constituents, Fluid Phase Equilibria 262 (2007) 187–209.
[40] W.V. Steele, R.D. Chirico, A.B. Cowell, S.E. Knipmeyer, A. Nguyen, Thermodynamic properties and ideal-gas enthalpies of formation for 2-aminoisobutyric acid (2-methylalanine), acetic acid, (Z)-5-ethylidene-2-norbornene, mesityl oxide (4-methyl-3-penten-2-one), 4-methylpent-1-ene, 2,2′-bis(phenylthio)propane, and glycidyl phenyl ether (1,2-epoxy-3-phenoxypropane), J. Chemical and Engineering Data 42 (6) (1997) 1053–1066.
[41] W.V. Steele, R.D. Chirico, S.E. Knipmeyer, A. Nguyen, Measurements of vapor pressure, heat capacity, and density along the saturation line for cyclopropane carboxylic acid, N,N-diethylethanolamine, 2,3-dihydrofuran, 5-hexen-2-one, perfluorobutanoic acid, and 2-phenylpropionaldehyde, J. Chemical and Engineering Data 47 (4) (2002) 715–724.
[42] D.C. Hanson, M.J. Van Winkle, J. Chemical and Engineering Data 12 (1967), cited in DECHEMA Data Series.
[43] V.V. Smirnov, S.Y. Pavlov, V.A. Groshkov, L.A. Serafimov, Prom-St. Sint. Kauch. 2 (1) (1976), cited in DECHEMA Data Series.
[44] Perry's, Chemical Engineer's Handbook, 6th ed., Mc Graw-Hill, 1984.
[45] M. Richter, H. Sovová, The solubility of two monoterpenes in supercritical carbon dioxide, Fluid Phase Equilibria 85 (1993) 285–300.
[46] M. Akgün, N. Akgün, S. Dincer, Phase behaviour of essential oil components in supercritical carbon dioxide, J. Supercritical Fluids 15 (1999) 117–125.
[47] E. Stahl, K.W. Quirin, Dense gas extraction on a laboratory scale: a survey of some recent results, Fluid Phase Equilibria 10 (1983) 269–278.
[48] H. Sovová, J. Jez, Solubility of menthol in supercritical carbon dioxide, J. Chemical and Engineering Data 39 (4) (1994) 840–841.
[49] H. Sovová, R.P. Stateva, A.A. Galushko, High-pressure equilibrium of menthol + CO_2, J. Supercritical Fluids 41 (2007) 1–9.
[50] M. Mukhopadhyay, S.K. De, Fluid phase behavior of close molecular weight fine chemicals with supercritical carbon dioxide, J. Chemical and Engineering Data 40 (1995) 909–913.
[51] M.L. Michelsen, The isothermal flash problem. Part II. Phase-split calculation, Fluid Phase Equilibria 9 (1982) 21–40.